

## Experimental Study for Heat Transfer Enhancement Due To Surface Roughness at Laminar Flow

Raju R.Yenare, Prof Kundlik V.Mali.

Department of Mechanical Engineering Sinhgad College of Engineering, Pune

Department of Mechanical Engineering Sinhgad College of Engineering, Pune

### Abstract

An investigation was conducted to determine whether dimples on a heat sink fin can increase heat transfer for laminar airflows. This was accomplished by performing experimental studies using two different types of dimples: 1) circular (spherical) dimples, and 2) oval (elliptical) dimples. Dimples were placed on both sides of a aluminium plate with a relative pitch of  $S/D=1.21$  and relative depth of  $\delta/D=0.16$  (e.g., circular dimples). For oval dimples, similar ratios with the same total depth and circular-edge-to-edge distance as the circular dimples were used. For those configurations the average heat transfer coefficient, pressure drop, thermal performance and Nusselt number ratio were determined experimentally. For circular and oval dimples, heat transfer enhancements (relative to a flat plate) were observed for Reynolds number range from 600 to 2000 (Reynolds number based on channel height). Also the results are validated analytically for Nusselt number and friction factor for plain vertical plate.

This experiment was undertaken to provide the needed experimental data that fill the gap for the use of dimples for laminar flow conditions. Specifically, this investigation was conducted to determine whether or not the use of dimples can enhance heat transfer characteristics for heat sink applications. Dimples enhanced heat transfer from its surface for laminar air flows while the pressure drop was equivalent or smaller than that of the flat surface. These surfaces do indeed enhance thermal performance without the penalty associated with higher pressure drops.

### I. INTRODUCTION

The importance of heat transfer enhancement has gained greater significance in such areas as microelectronic cooling, especially in central processing units, macro and micro scale heat exchangers, gas turbine internal airfoil cooling, fuel elements of nuclear power plants, and bio medical devices. A tremendous amount of effort has been devoted to developing new methods to increase heat transfer from fined surface to the surrounding flowing fluid. Rib tabulator, an array of pin fins, and dimples have been employed for this purpose.

In case of the electronics industry, due to the demand for smaller and more powerful products, power densities of electronic components have increased. The maximum temperature of the component is one of the main factors that control the reliability of electronic products. Thermal management has always been one of the main issues in the electronics industry, and its importance will grow in coming decades.

The use of heat sinks is the most common application for thermal management in electronic packaging. Heat sink performance can be evaluated by several factors: material, surface area, flatness of contact surfaces, configuration, and fan requirements. Aluminum is the most common material because of its high conductivity (205W/mK), low cost, low

weight, and easiness with respect to manufacturability. Copper is also used for heat sinks because of very high conductivity (400W/mK), but its disadvantages include high weight, high price, and fewer choices as far as production methods. To combine the advantages of aluminum and copper, heat sinks can be made of aluminum and copper bonded together. To improve performance, heat sinks should be designed to have a large surface area since heat transfer takes place at the surface. In addition, flatness of the contact surface is very important because a nominally flat contact area reduces the thermal interface resistance between the heat sink and heat source. A heat sink must be designed to allow the cooling fluid to reach all cooling fins and to allow good heat transfer from the heat source to the fins. Heat sink performance also depends on the type of fluid moving device used because airflow rates have a direct influence on its enhancement characteristics.

To obtain higher performance from a heat sink, more space, less weight, and lower cost are necessary. Thus, efforts to obtain more optimized designs for heat sinks are needed to achieve high thermal performance.

One method to increase the convective heat transfer is to manage the growth of the thermal boundary layer. The thermal boundary layer can be made thinner or partially broken by flow disturbance.

As it is reduced, by using interrupted and/or patterned extended surfaces, convective heat transfer can be increased. Pin fins, protruding ribs (turbulators), louvered fins, offset-strip fins, slit fins and vortex generators are typical methods. The pattern and placements are suitably chosen based on the required cooling.

Generally, heat transfer augmentation techniques are classified in three broad categories: active methods, passive method and compound method. Following are the some of experimental studies.

**Chyu et al.** [2] studied the enhancement of surface heat transfer in a channel using two different concavities- hemispheric and tear drop. Concavities serve as vortex generators to promote turbulent mixing in the bulk flow to enhance the heat transfer at  $Re_H = 10,000$  to  $50,000$ ,  $H/d$  of 0.5, 1.5, 3.0 and  $\delta/d = 0.575$ . Heat transfer enhancement was 2.5 times higher than smooth channel values and with very low pressure losses that were almost half that caused by conventional ribs turbulators.

**Moon et al.** [3] experimentally studied the effect of channel height on heat transfer performance and friction losses in a rectangular dimpled passage with staggered dimples on one wall. The geometry used was  $H/D = 0.37, 0.74, 1.11, 1.49$  and  $Re_H = 12,000$  to  $60,000$ . Heat transfer enhancement was roughly 2.1 times greater than the smooth channel configuration with  $H/D$  values from 0.37 to 1.49. The heat transfer augmentation was invariant with the Reynolds number and channel height. The increase in friction factor was 1.6 to 2.0 times less than the smooth channel. The pressure losses also remained approximately constant for the channel height.

**Mahmood et al** [4] studied the flow and heat transfer characteristics over staggered arrays of dimples with  $\delta/D=0.2$ . For the globally average Nusselt number, there were small changes with Reynolds number. Ligrani et al [5] studied the effect of dimpled protrusions (bumps) on the opposite wall of the dimpled surface.

**Mahmood et al** [6] experimentally showed the influence of dimple aspect ratio, temperature ratio, Reynolds number and flow structures in a dimpled channel at  $Re_H = 600$  to  $11,000$  and air inlet stagnation temperature ratio of 0.78 to 0.94 with  $H/D = 0.20, 0.25, 0.5, 1.00$ . The results indicated that the vortex pairs which are periodically shed from the dimples become stronger and local Nusselt number increase as channel height decreases. As the temperature ratio  $T_{oi}/T_w$  decreases, the local Nusselt number also increased.

**Burgess et al** [7] experimentally analyzed the effect of dimple depth on the surface within a channel with the ratio of dimple depth to dimple printed diameter, equal to  $\delta/D, 0.1, 0.2, \text{ and } 0.3$ . The data showed that the local Nusselt number increased as the dimple depth increased due to an increased strength and intensity of vortices and three dimensional (3D) turbulent productions. Ligrani et al studied the effect of inlet turbulence level in the heat transfer improvement in walls with dimple ratio  $\delta/D=0.1$ , showing that as the turbulence level was increased, the relative Nusselt number reduced due to the increased turbulent diffusion of vorticity.

**Bunker et al** [8] use circular pipes with in-line arrays of dimples with  $\delta/D=0.2$  and  $0.4$  and surface area densities ranging from 0.3 to 0.7 to provide heat transfer enhancement and friction effects of dimples in a circular tube. Reynolds numbers for bulk flow were from 20,000 to 90,000. Heat transfer enhancement was 2times greater than the smooth circular tube in the case where the relative dimple depth was greater than 0.3 and array density was greater than 0.5. An increase of friction factor was approximately 4 to 6 times greater than the smooth circular tube, which was better than the rib turbulators. Han studied the rotational effect of dimples in turbine blade cooling. In the case where a pressure drop is the main design concern, dimple cooling can be a good choice. Jet impingement over a convex dimpled surface was studied by Chang et al. [9] showing an incremental increase in the relative Nusselt number ( $N_u/N_{u0}$ ) up to 1.5.

In this experimental work the heat transfer coefficient  $h$  is increase by using the various dimple plate such as circular and oval. These experimental studies are carried out at laminar flow for the Reynolds number 600 to 2000.

## II. EXPERIMENTAL WORK

### 2.1 Experimental Setup.

In the experimental set up blower, digital flow meter, plenum ,acrylic glass channel test section with aluminium plate and control panel consist of temperature indicator, voltmeter, ammeter , dimmer stat are used

An experimental set up is used for finding the necessary data for obtaining Nusselt number is shown in Fig.1 The average heat transfer coefficient on the plate surface will be measured for various rates of airflow through the channel. It consists of an open loop flow circuit. The main components of the test apparatus are a test section, a rectangular channel, a plenum, a calibrated digital flow meter, a ball valve, and a centrifugal blower. The channel inner cross section dimensions are 33 mm (wide) and 105 mm (height). The entrance channel is 2500 mm long. The channel is constructed with 8 mm thick

acrylic plates with thermal conductivity  $k=0.16W/mK$  at  $20^{\circ}C$  to minimize heat losses. A  $300X300X450$  mm plenum with wood will be fabricated to stabilize the flow drawn by the blower.



Fig .1 Experimental set up

### 2.2 Details of test section

The circular dimpled plate with 12 by 24 dimples is shown in figure 2 and figure 3 shows the oval (elliptical) dimpled plate with 7 by 24 dimples on each side. The dimples were placed on both sides of the test plate with a relative pitch  $S/D=1.2$  and a relative depth  $\delta/D=0.166$  for the circular dimples. For the oval dimples,  $S/D=1.2$  and  $\delta/D=0.166$  with same total depth and circular-edge-to-edge distance as the circular dimples. Three test plates were fabricated with 5mm thickness Aluminum. Because a flat projected area is used to calculate a heat transfer coefficient and a Nusselt number, the total surface area for each plate is constant.

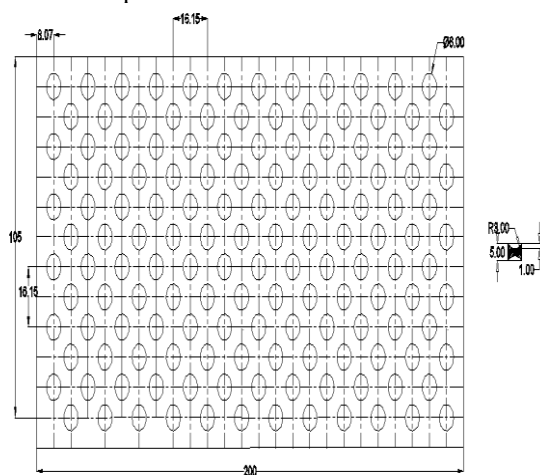


Fig 2. details of circular dimple plate.

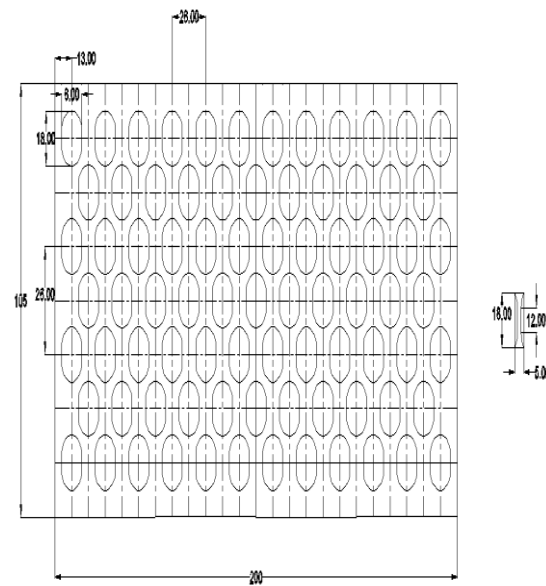


Fig 3.details of oval dimple plate.

### 2.3 Experimental Procedure.

The test plate is located in the middle of the test channel. Care was taken so that the test plate can be located in the middle of the test section in order to ensure an equal channel height conditions and airflow rates for both sides of the test plate. The outer surface of the test section consisted of fiberglass to reduce heat loss to the outside surroundings.

The blower is turned on and air is forced through the test setup. The flow rate through the test section is controlled with the help of a valve downstream of the digital flow meter. The flow rate is set in such a way so that the pressure drop across the orifice corresponds to required Reynolds number.

After the flow is set across the test section, the heater is turn on and the voltage supplied to the heater is roughly set to 15W. According to the temperature of the test plate, voltage and current is changed. After the measured temperatures are reached a specific value, the voltage is controlled to an input power 12W.

After as time elapse of roughly 6 hours approximately, the temperature of the test plate reaches steady state. The pressure difference across the test section is checked frequently so that the flow rate does not change from the intended value of Reynolds number. At steady state, the temperatures of the test plate are checked by the observation. The pressure difference across the test plate and the pressure across upstream of the test plate is measured. The voltage supplied to the heater and the corresponding current is taken to calculate the heat supplied to the test plate. The temperatures of the inlet air into the test section and outlet section also checked.

**2.4 Data reduction**

The data reduction of the measured results is summarized in the following procedures

An average heat transfer coefficient is calculated from the net heat transfer per unit area, the average temperature of the plate, and the bulk mean air temperature. To quantify the average heat transfer coefficient, the following expression can be used:

$$h = \frac{Q_{net}}{A_s(T_w - T_b)} = \frac{Q_{total} - Q_{loss}}{A_s(T_w - T_b)} \quad \dots (1)$$

Where the net heat flux ( $Q_{net}$ ) is the electrical power supplied to the heater ( $Q_{total}$ ) minus the heat loss from the test section ( $Q_{loss}$ ).  $A_s$  is the surface area of the plate where the heat convection occurs.  $T_w$  is a steady-state wall temperature and  $T_b$  is a mean bulk temperature.

$$Q = V * I \quad \dots (2)$$

For the general case, heat loss is calculated to be roughly 10 to 20%.

A mean bulk temperature,  $T_b$ , is determined by Eq. 3 where  $T_{b, inlet}$  is the inlet bulk temperature and  $T_{b, outlet}$  is the outlet bulk temperature that can be calculated from Eq.3 while the wall temperature is calculated by equation 4.

$$T_b = \frac{T_{b, inlet} + T_{b, outlet}}{5} \quad \dots (3)$$

$$T_w = \frac{(T_1 + T_2 + T_3 + T_4 + T_5)}{5} \quad \dots (4)$$

Where  $T_1, T_2, T_3, T_4, T_5$  are the wall temperature measured with the help of temperature indicator.

a) The Nusselt number for heat transfer over the vertical plate

$$Nu = 0.228 Re^{0.731} Pr^{0.33} \quad \dots (5)$$

b) Nusselt number

$$Nu = \frac{hL_c}{K} \quad \dots (6)$$

$$Pr = \frac{Cp\mu}{K} \quad \dots (7)$$

d) Reynolds number

$$Re = \frac{\rho V D}{\mu} \quad \dots (9)$$

e) Pressure drop for laminar flow

$$\Delta P = \frac{(f * L * \rho * V^2)}{2 * d} \quad \dots (10)$$

f) Friction factor for laminar flow

$$f = \frac{68.36}{Re} \quad \dots (11)$$

**III. RESULTS AND DISCUSSION**

Experimentally determined Nusselt number values for plain plate without dimple are compared with analytical equation of Nusselt number over the vertical plate at laminar flow

The comparison between Nusselt numbers obtained experimentally and by using theoretical Nusselt number equation for plain vertical plate is as shown in figure.7. It is observed that the value of Nu (experimental) is less than Nu (theoretical). Actual heat carried away by air passing through the test section is the combination of convective and radiative heat transfers. As the heat transferred by convection alone is considered while performing experimental calculations, it can be expected that Nu (experimental) is less than Nu.

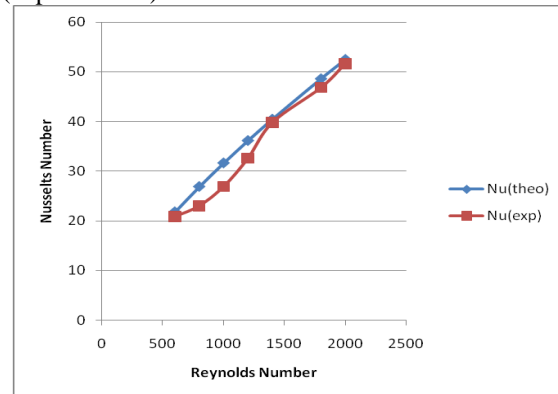


Fig.7 Comparison between Nusselts numbers obtained experimentally and analytically.

The variation of friction factor with Reynolds number for plain plate is shown in figure 5. The data obtained by the experiment is compared with friction factor obtained analytically by equation for laminar flow over a vertical flat plate for less than 2300 Reynolds number. The friction factor value obtained by experiment is higher than theoretical friction factor. The friction factor is high at low Reynolds number and it increase with increase in Reynolds number

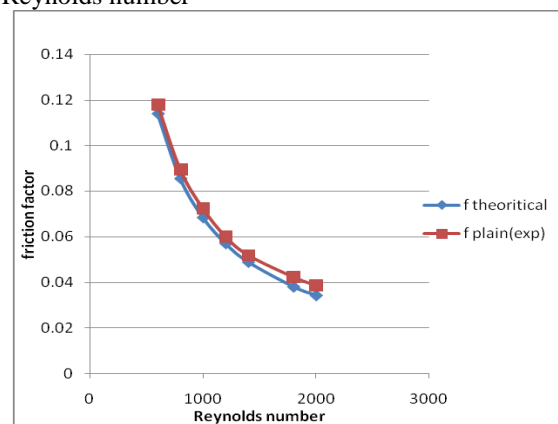


Fig.5 Validation of numerical results for friction factor of plain plate against existing correlation

The heat transfer coefficients for three different aluminum plates based on the flat projected is shown in figure.6. The heat transfer coefficients increased with increasing airflow rate. The results showed that the heat transfer coefficients for the

circular and oval dimpled plates were higher than that of the flat plate for all airflow conditions. For Reynolds number 600 the increase in heat transfer coefficient is from 2.6063 for the plain plate to 2.8834 for oval plate. While at higher Reynolds number 2000 the heat transfer coefficient is 6.7063 for plain plate which increase to 8.4091 for the oval plate.

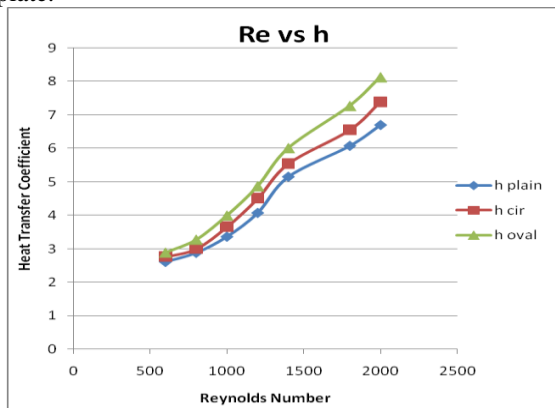


Fig.6. Heat Transfer coefficient for the different aluminum plates

Fig.8 compares the thermal performance factor for two different dimpled plates: circular and oval dimpled plate. Both cases showed that the thermal performance factor increases with increasing mass flow rate. The thermal performance factor for the oval dimpled plate increased from 1.0 to 1.114. The thermal performance factor for the circular dimpled plate increased from 1.0 to 1.05. The factor for the oval type dimpled plate was larger than that of the circular dimpled plate for all cases.

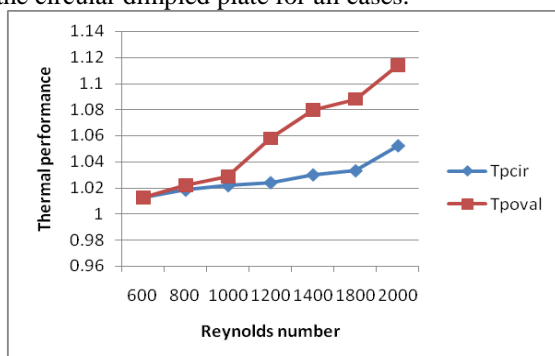


Fig.8 Thermal performance for circular and oval dimpled plate

Experimental investigations of heat transfer, friction factor and thermal enhancement factor of a plain plate with circular and oval plate are described in the present in the report. The conclusions can be drawn as follows:

1. The heat transfer enhancement increases for an oval plate over the circular plate and plain plate . This is due to increases in the turbulence of air

provided by the oval plate is more as compared to plain and circular dimple.

2. The friction factor increases for an oval plate over the circular plate and plain plate a again due to more swirl flow exerted by the oval plate.
3. The enhancement of Nusselt number is much higher than that of enhancement in friction factor for all the types of circular and oval plate justifies its use for heat transfer at laminar flow.
4. The pressure drops of the dimpled plates for a laminar airflow are either equivalent to, or less than values produced in a flat plate with no dimples. The pressure drop of the oval type dimpled plate is smaller than that of the circular type dimpled plate.

## REFERENCES

- [1] P.W. Bearman and J.K. Harvey, Control of circular cylinder flow by the use of dimples, AIAA J. 31 (1993) 1753-1756.
- [2] M.K. Chyu, Y. Yu, H. Ding, J.P. Downs and F.O. Soechting, Concavity enhanced heat transfer in an internal cooling passage, International Gas Turbine & Aeroengine Congress & Exhibition ASME paper 97-GT-437.
- [3] H.K. Moon, T. O`Connell and B. Glezer, Channel height effect on heat transfer and friction in a dimpled passage, J. Gas Turbine Power 122 (2000) 307-313.
- [4] G.I. Mamood, M.L. Hill, D.L. Nelson, P.M. Ligrani, H.K. Moon and B. Glezer, Local heat transfer and flow structure on and above a dimpled surface in a channel, J. Turbomachinery 123 (2001) 115-123.
- [5] P.M. Ligrani, G.I. Mamood and M.Z. Sabbagh, Heat transfer in a channel with dimples and protrusion on opposite walls, J. Thermophys. Heat Transfer 15 (3) (2001) 275-283.
- [6] G.I. Mahmood and P.M. Ligrani, Heat Transfer in a dimpled channel: combined influences of aspect ratio, temperature ratio, Reynolds number, and flow structure, Int. J. heat Mass Transfer 45 (2002) 2011-2020.
- [7] N.K. Burgess and P.M. Ligrani, Effects of dimple depth on channel nusselt numbers and friction factors, J. Heat Transfer 127 (8) (2005) 839-847.
- [8] R . S. Bunker and K.F. Donellan, Heat transfer and friction factors for flow inside circular tubes with concavity surfaces, J. Turbomachinery 125 (4) (2003) 665-772.
- [9] S.W. Chang, Y.J. Jan and S.F. Chang, Heat transfer of impinging jet-array over convex-dimpled surface, Int. J. Heat Mass Transfer 49 (2006) 3045-3059.